Eur Radiol (2013) 23:65–74
DOI 10.1007/s00330-012-2575-2

MAGNETIC RESONANCE

ADC maps in the prediction of pelvic lymph nodal metastatic regions in endometrial cancer

Gilda Rechichi · Stefania Galimberti · Matteo Oriani · Patrizia Perego · Maria Grazia Valsecchi · Sandro Sironi

Received: 7 April 2012 / Accepted: 31 May 2012 / Published online: 21 July 2012

Abstract
Objectives To evaluate the usefulness of apparent diffusion coefficient (ADC) in discriminating metastatic from non-metastatic pelvic lymph nodal sites in endometrial cancer.
Materials and methods This retrospective study included 40 patients with endometrial cancer who underwent MRI [T2-weighted, dynamic T1-weighted images and diffusion-weighted images with body background suppression (DWIBS), b-values 0 and 1,000 s/mm^2], total hysterectomy and pelvic lymphadenectomy. Lymph nodes identifiable on DWIBS were evaluated, classified into six nodal regions, and for each node ADC values, short- and long-axis diameters were measured by two readers. Histopathological findings and follow-up information served as the reference standard.

Results Average (± standard deviation) mean and minimum ADC region value (0.87 ± 0.15 and $0.74\pm0.07\times10^{-3}$ mm^2/s) of metastatic sites ($n=7$) were significantly lower than those of non-metastatic ones ($n=89$; 1.07 ± 0.20 and 1.02 ± 0.20; p-value=0.010 and 0.0004). Mean short-axis and short-to-long axis ratios of metastatic nodes were 7.47 mm and 0.68. Using the minimum ADC region value with threshold 0.807×10^{-3} mm^2/s, sensitivity, specificity, positive and negative predictive value and accuracy were 100 %, 98.3 %, 63.6 %, 100 % and 98.3 %, respectively (reader 1).
Conclusion In endometrial cancer, mean and minimum ADC region values of metastatic nodal sites are significantly lower than those found at normal sites.
Key Points
- *Magnetic resonance imaging is widely used for endometrial cancer.*
- *Nodes involved with metastases show lower ADC values than normal nodes.*
- *ADC values show higher diagnostic performances than conventional size criteria.*
- *Minimum region ADC values perform better than mean region ADC values.*
- *The radiologist can indicate to the surgeon which nodal stations are involved.*

Keywords Diffusion · ADC · MRI · Endometrial cancer · Lymph nodes

Electronic supplementary material The online version of this article (doi:10.1007/s00330-012-2575-2) contains supplementary material, which is available to authorized users.

G. Rechichi · S. Galimberti · M. Oriani · M. G. Valsecchi · S. Sironi
School of Medicine, University of Milano-Bicocca, Milan, Italy

G. Rechichi (✉) · M. Oriani · S. Sironi
Department of Diagnostic Radiology, H S. Gerardo Monza, MB, Via Pergolesi 33, 20900 Monza, MB, Italy
e-mail: gilda.rechichi@gmail.com

S. Galimberti · M. G. Valsecchi
Department of Clinical Medicine and Prevention—Centre of Biostatistics for Clinical Epidemiology, University of Milano-Bicocca, Milan, Italy

P. Perego
Department of Pathology, H.S. Gerardo Monza, Milan, Italy

Introduction

Prognosis of endometrial cancer has been directly correlated to the surgical findings including the final tumour grade, depth of myometrial invasion and lymph node metastases [1]. In particular, the presence of lymph node metastasis is

an important issue for patients with cervical and uterine cancers, since it influences the 5-year survival and affects treatment planning [2, 3]. A threshold diameter of 10 mm in the short axis is commonly applied in magnetic resonance (MR) imaging to distinguish metastatic from benign nodes, but it appears to be rather accurate, with low sensitivities ranging from 24 % to 73 %, despite higher corresponding specificities ranging from 93 % to 97 % [4–6]. In this regard, it has therefore been suggested that functional approaches may allow a more reliable determination of malignant nodal involvement than the classical morphological assessment [6].

Diffusion-weighted magnetic resonance (DW MR) imaging is a noninvasive imaging tool primarily based on functional rather than morphologic criteria. It derives its image contrast from the random diffusion motion of water molecules [7, 8]. The extent of water diffusion can be related to microstructure, microcirculation, cell organisation and density, thus allowing DWI to provide information about the biophysical properties of tissues in vivo [6]. The apparent diffusion coefficient (ADC) is a quantitative parameter describing the microscopic water diffusivity [7], and it relates to the translational movement of water molecules, which is limited in an environment that contains structures such as cell membranes. Because malignant tumours generally have higher cellularity than benign lesions, ADC values might theoretically assist in differentiating malignant from benign lesions [9–12].

In previous studies, it has been suggested that ADC may improve the diagnostic performance of MR in the detection of metastatic lymph nodes in several different malignancies on the basis of lower ADC values in cancerous than in non-cancerous nodes [7, 13–18]. However, only few papers have investigated the reliability of DWI in the evaluation of lymph node status in patients with endometrial cancer, with wide discrepancies existing between the reported results [6, 16, 19].

The purpose of the present study was to evaluate the usefulness of the apparent diffusion coefficient (ADC) derived from diffusion weighted images with body background suppression (DWIBS) in discriminating metastatic from non-metastatic pelvic lymph nodal sites in endometrial cancer patients.

Materials and methods

Study population

This retrospective study, carried out at our institution (November 2008–May 2011), included 64 consecutive patients with histologically confirmed endometrial adenocarcinoma. They all underwent MRI as part of the standard pre-operative protocol and subsequent total hysterectomy. Patients were excluded if: lymphadenectomy was not performed (n=16); they were treated with preoperative chemotherapy/radiotherapy (n=4); they had metal pelvic/hip prostheses (n=1); they were unable to cooperate or claustrophobic (n=3). Of the patients initially considered, 40 were finally enrolled in the study. They had a mean age of 56 years (range: 45–69) and were mostly post-menopausal (82.5 %).

All patients provided written informed consent to participate. Approval from our Institutional Review Board was obtained.

MR imaging protocol

MR examinations were performed with a 1.5-T system (Achieva Plus; Philips, The Netherlands), with a phased SENSE five-channel phased-array cardiac coil and a Q-body coil. The MR imaging protocol consisted of four sequences.

(1) T1-weighted turbo spin-echo images: axial plane (FOV: 375×264 mm; TE: 4.6 ms; TR: 4.4 ms; slice thickness: 7 mm; slice gap: 1 mm; matrix: 256×143).
(2) T2-weighted turbo spin-echo images: sagittal and oblique axial planes (FOV: 177×105 mm; TE: 85 ms; TR: 5,000 ms; slice thickness: 3 mm; slice gap: 0.3 mm; matrix: 361×198); oblique coronal plane (FOV: 220×177 mm, matrix: 368×215). The oblique axial and coronal planes were placed in relation to the minor/major axis of the uterine body.
(3) Diffusion-weighted images with echo-planar technique with body background suppression (FOV: 400×280 mm; TE: 70 ms; TR: 9,344 ms; slice thickness: 4 mm; b-value of 0 and 1,000 s/mm^2; matrix: 160×87; number of signals averaged: 10; acquisition time: 6.32 min): axial plane under free breathing. DWIBS were not fused with other images (i.e. T2-weighted) [6, 16].
(4) Contrast-enhanced fat-suppressed T1-weighted images (FOV: 395×280 mm; TE: 2.1 ms; TR:4.3 ms; slice thickness: 2 mm; matrix: 256×196): axial plane, after administration of gadopentate dimeglumine (Magnevist; Schering, Berlin, Germany; 0.2 ml/kg body weight; injection flow 2 ml/s), followed by a 20 ml saline flush; images obtained at 0, 30, 60 and 120 s after injection of the contrast agent.

MR image analysis

Two radiologists (7- and 5-year experience in gynaecological MR imaging) independently evaluated all sequences performed in each patient. They were blinded to clinical data, apart from the presence of endometrial cancer, and to the results of the postoperative histopathological examination. ADC maps were generated using the standard software on

Table 1 Relevant clinical and histopathological data on 40 patients with endometrial cancer who underwent total hysterectomy and pelvic bilateral lymphadenectomy

Characteristic	*n* (%)
Menopause	
No	7 (17)
Yes	33 (83)
Istotype	
Endometrioid	36 (90)
Squamous	2 (5)
Serous (rev 2; point 6)	2 (5)
Histologic tumour grade*	
G1	8 (20)
G2	23 (58)
G3	9 (22)
Depth of myometrial invasion (%)	
0–50	28 (70)
≥50	12 (30)

*G1, well differentiated; G2, moderately differentiated; G3, poorly differentiated

the scanner console on a pixel-by-pixel basis with a mono-exponential fit from DW images. Contrast-enhanced, T2-weighted DWIBS images and ADC maps were read in parallel. Oblique axial T2-weighted and axial contrast-enhanced images were used to determine the size and location of lymph nodes [6, 16].

In agreement with previous authors [6], pelvic nodal sites were classified into six regions: common iliac, external iliac and internal iliac-obturator nodes, both right and left. In these locations, all hyperintense nodes on DWIBS images (b-value=1,000 s/mm^2) were considered for ADC measurements [16]. The two radiologists manually placed irregular regions of interest (ROI) on DWIBS images [20] that contained the largest nodal area, so that the largest ROI could be drawn within the targeted tissues [21]. The ROI was subsequently copied to the corresponding ADC map [7] and for each identifiable node ADC measurements were obtained.

In the axial contrast-enhanced and oblique axial T2-weighted images, the largest short-axis and long-axis diameters of each identifiable node were observed and recorded; the short-to-long axis ratio was also calculated [21].

Surgical procedure and histopathological analysis

Total hysterectomy and pelvic bilateral lymphadenectomy were performed in all patients 7–15 days after MRI examination (mean wait: 11 days). The surgical procedure was performed by two gynaecological surgeons (more than 10 years of experience each). They carefully searched for any possible metastases at the pelvic lymph node dissection [6], based on histopathological biopsy-proven data and prior partial knowledge of MRI (regarding myometrial invasion and tumour grading), being unaware of the results of ADC measurements.

The resected nodes were anatomically labelled by the surgeons into the same six regions as for MR analysis and were sectioned and evaluated by a pathologist (15 years of experience in gynaecological oncology), who was blinded to imaging results. The histopathological report included the number of total dissected nodes and of the metastatic ones in each region [6, 21]. For each metastatic lymph node, its long- and short-axis diameters were also recorded.

Statistical analysis

The diagnostic ability of ADC in the classification of lymph node metastases was evaluated on a region-based analysis. The reference standards were histopathological results for

Table 2 Results of the (a) histopatological and (b) MRI findings, classified according to pelvic regions

Findings	Regions												Total	
	Right						Left							
	Common iliac		External iliac		Internal iliac-obturator		Common iliac		External iliac		Internal iliac-obturator			
	No. pts	No. lymp	No. pts	No. lymp	No. pts	No. lymp	No. pts	No. lymp	No. pts	No. lymp	No. pts	No. lymp	No. pts	No. lymp
(a) Histopatological														
- Pathologist	14	48	33	203	33	150	11	41	34	182	36	191	40	815
- Observed metastasis	0	0	1*	1	0	0	0	0	5*	9	1	5	6	15
(b) MRI														
- Reader 1	5	5	34	70	15	18	5	6	34	75	18	31	40	205
- Reader 2	5	5	34	71	15	18	5	6	34	70	17	27	40	197

*One patient has two regions involved

Legend: pts = patients; lymp = lymph nodes

resected regions and follow-up information for non-resected regions (a region was considered free from nodal disease if it had no signs of metastases at clinical evaluation and at pelvic MR or PET/CT scan 6 months after surgery).

The ADC values obtained from all the hyperintense lymph nodes detected on DWIBS in each region were summarised using both the mean and the minimum [16]. As the estimate of the intra-patient correlation index, which quantifies the degree of dependence of region values within patients, was close to zero in both readers and measures, standard approaches for independent data were used for the analyses. The interobserver agreement for the region ADC summary measures was analysed according to the Bland-Altman method. The comparison of the average ADC region values in groups identified by metastatic status was performed using the t-test (two-sided, α=0.05).

For both the mean and the minimum ADC region values, the cutoff discriminating metastatic from non-metastatic sites was calculated maximising the Youden index on the receiver operating characteristics (ROC) curve. Different MR diagnostic criteria based on the T2 protocol, such as the short axis (≥10 mm) and short to long axis ratio (>0.77), were also considered. Indices of diagnostic performances were calculated together with their 95 % confidence intervals (CI), determined based on asymptotics or on the Wilson approach [22], when appropriate.

Results

Histopathological findings

The majority of the 40 women included in this study presented with tumours of endometrioid istotype (90 %), moderately differentiated (G2) (58 %), and with absent or superficial myometrial invasion (70 %), as reported in Table 1.

A total of 161 nodal regions were dissected by the surgeons and evaluated by the pathologist, with a mean of four regions per patient (range: 1–6). These regions included a total of 815 lymph nodes (mean of 20.4 nodes per patient, range: 4–45), of which 15 were metastatic (1,8 %) in 7 regions, in 6 patients. Five out of these patients (83.3 %) had moderately or poorly differentiated endometrial tumour (G2 or G3) and/or myometrial invasion >50 %. As reported in Table 2(a), 726 out of 815 nodes (89 %) were located in both the right and left common and external iliac regions. The majority of metastatic nodes were located in the left external iliac region (9 out of 15 nodes, 60 %), but metastases were found also in the right external iliac region (1 out of 15, 7 %) and in the left internal iliac and obturator region (5 out of 15, 33 %). The mean short-axis diameter (mm) and short-to-long axis ratio of metastatic nodes were 7.47 mm (range: 4–17 mm) and 0.68 (range: 0.27–1), respectively.

Among non-metastatic lymph nodes, 62 (7.6 %) were recorded as reactive benign nodes, and they were observed in only 2 patients. It has to be noted that in these two patients all resected nodes were found to be reactive, without any normal or metastatic nodes.

The status of the 79 non-dissected regions that, added to the 161 dissected by the surgeon, constituted the total of 240 analysed sites was derived from follow-up. As none of the patients had pelvic metastatic involvement in the 6 months after surgery, we assumed that the 79 nodal regions were free from metastases.

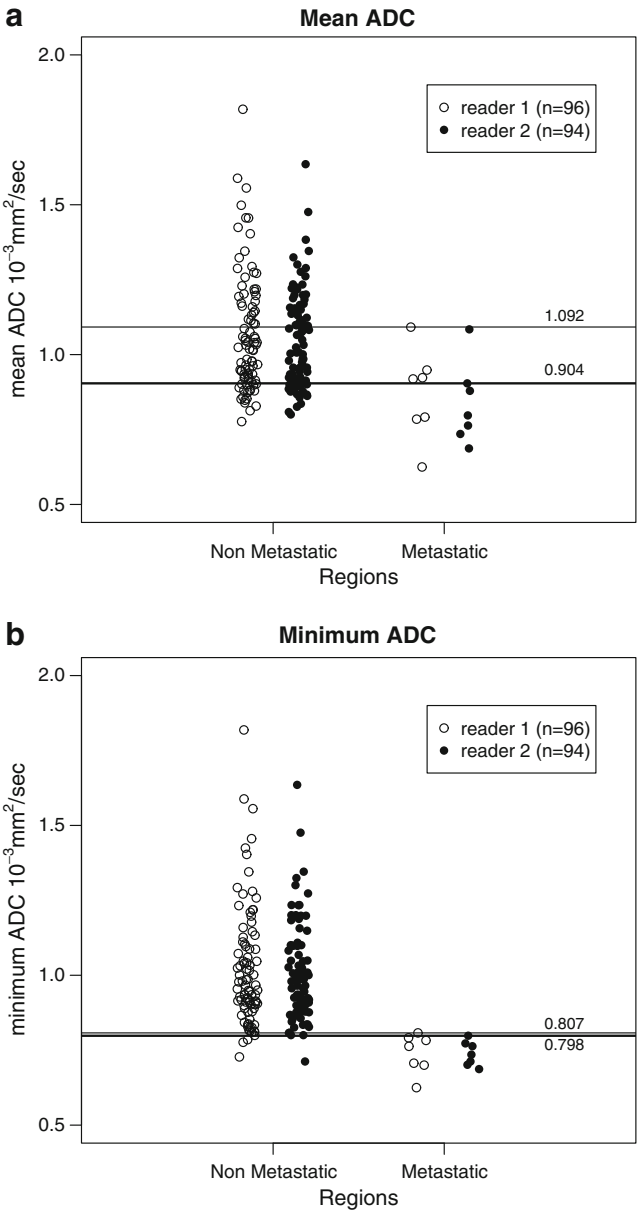

Fig. 1 **a**–**b**: **a** Mean and **b** minimum ADC values of regions with histopatologic data by metastatic status and reader. The horizontal lines represent the cutoff values that discriminate metastatic from non-metastatic pelvic regions for reader 1 (thin line) and reader 2 (solid line)

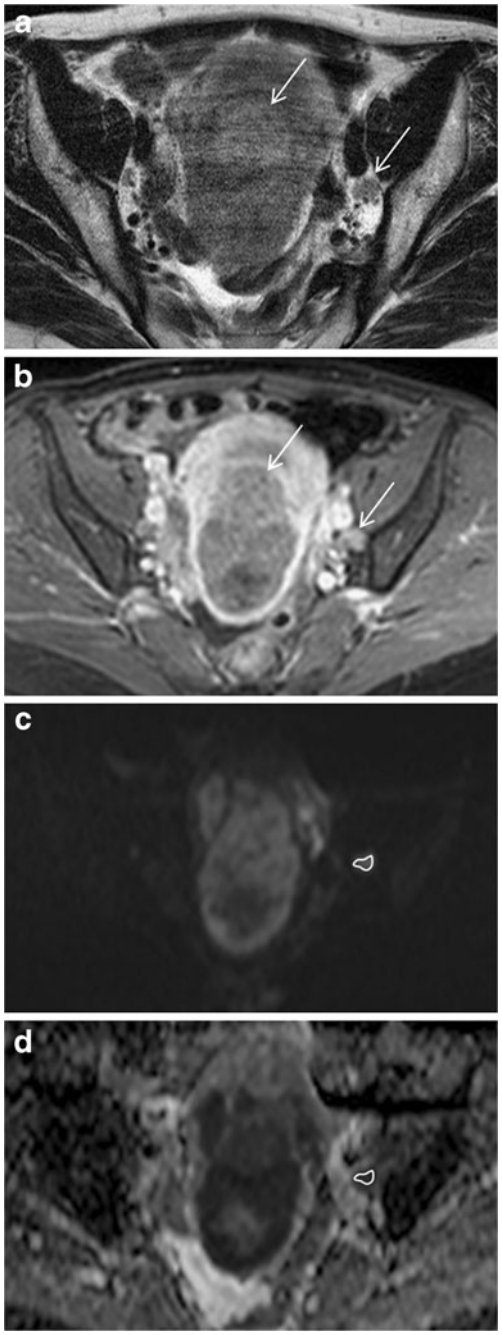

Fig. 2 **a**–**d**: MR images of a 56-year-old woman with endometrial cancer. At post-operative histopathological analysis, metastatic nodes were found in the left internal iliac-obturator region. **a** Oblique axial T2-weighted image (TE: 85 ms; TR: 5,000 ms) shows a neoplastic mass filling the uterine cavity (thin arrow) and an enlarged lymph node in the left internal iliac-obturator region (thick arrow), suspected as metastatic. **b** Contrast-enhanced axial T1-weighted image (TE: 2.1 ms; TR: 4.3 ms) confirms the presence of the uterine tumour (thin arrow) and of the enlarged node (thick arrow), with heterogeneous enhancement. **c** Both the tumour and the node show high signal intensity on DWIBS image with b-value=1,000 s/mm^2 (TE: 70 ms; TR: 9,344 ms); a ROI is set into the enlarged node. **d** ADC map, where the ROI was copied

MR findings

A total of 205 hyperintense lymph nodes (mean of 5.1 nodes per patient, range of 2–12) were identified on DWIBS images in 111 nodal regions by reader 1, while 197 lymph nodes

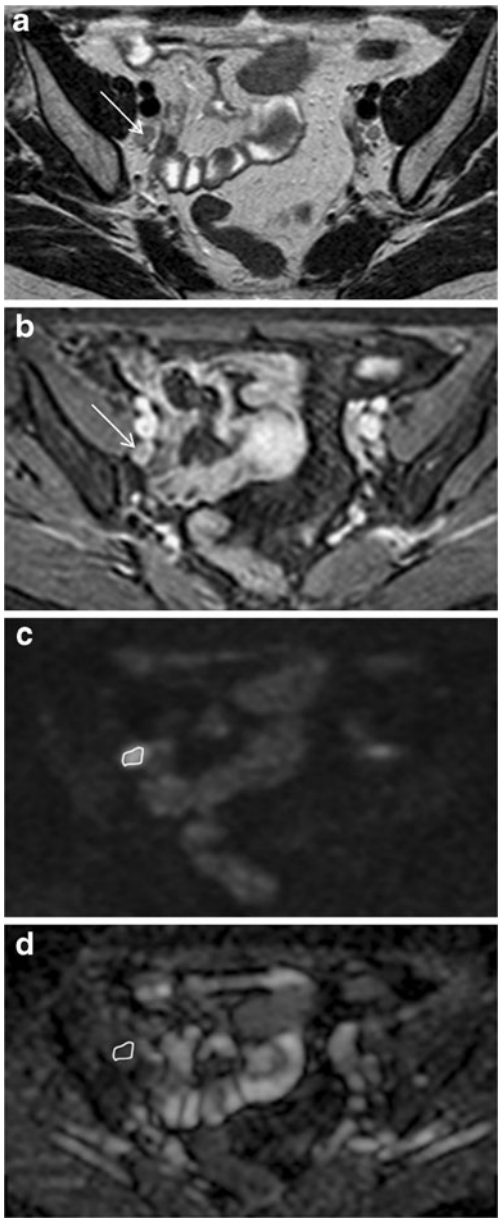

Fig. 3 **a**–**d**: MR images of a 51-year-old woman with endometrial cancer. At post-operative histopathological analysis, no metastatic nodes were found in any of the dissected nodal regions (n=6). **a** Oblique axial T2-weighted image (TE: 85 ms; TR: 5,000 ms) shows an enlarged lymph node in the right external iliac region (arrow), suspected as metastatic. **b** Contrast-enhanced axial T1-weighted image (TE: 2.1 ms; TR: 4.3 ms) confirms the presence of the the enlarged node (arrow), with heterogeneous enhancement. **c** The lymph node appears hyperintense on DWIBS image with b-value=1,000 s/mm^2 (TE: 70 ms; TR: 9,344 ms), and a ROI is set into the node itself. **d** ADC map, where the ROI was copied

(mean of 4.9 nodes per patient, range 2–11) in 110 regions by reader 2. Detailed results about locations of the observed nodes for the two readers are shown in Table 2(b). They reflect the same pattern observed by the pathologist. There was an almost perfect agreement between the two readers in the identification of the regions with hyperintense lymph nodes, as among the 111 and 110 pelvic nodal regions evaluated for the quantitative assessment of ADC, 109 were in common. As for the ADC region-based values, the two readers tended to disagree only for higher values of ADC (Supplementary Figure 1a, b). However, when the Bland-Altman analysis was performed on values below 1.3×10^{-3} mm^2/s, the agreement between the two readers was uniform and the bias was low: -0.009×10^{-3} mm^2/s, (limits of agreement: −0.113; 0.097) and -0.003×10^{-3} mm^2/s (limits of agreement: −0.114; 0.107) for the mean and the minimum ADC region values, respectively (Supplementary Fig. 2a, b).

The average (± SD) of the mean ADC region values observed by reader 1 in the seven metastatic regions was 0.87±0.15 (10^{-3} mm^2/s), while for the minimum ADC region value, it was 0.74±0.07 (10^{-3} mm^2/s). The corresponding findings for the 89 non-metastatic regions were 1.07±0.20 and 1.02±0.20, respectively. The average ADC values of metastatic and non-metastatic regions were significantly different both for the mean (p-value=0.0103) and the minimum (p-value=0.0004) ADC region values (Figs. 1, 2 and 3). Similar findings were observed for reader 2, as shown in Table 3. These results were obtained from the subset of 96 and 94 pelvic nodal regions, with both histopatological and MR data, out of 111 and 110 respectively evaluated by the two readers. The remaining 15 and 16 nodal stations were free from metastases at follow-up and, when added to data obtained from the pathologist to reach the total observed regions, the significant difference in ADC values remained (Supplementary Table 1).

ROC analysis produced the following results: the cutoffs for the mean ADC region value were 1.092 and 0.904 (10^{-3} mm^2/s) for reader 1 and 2, respectively, while the thresholds for the minimum ADC region value were 0.807 and 0.798 (10^{-3} mm^2/s), respectively (Fig. 4). Table 4 shows the indices of diagnostic performance for the mean and minimum ADC region values and for the standard size criteria.

In particular, using a mean ADC region value of 1.092×10^{-3} mm^2/s as threshold in order to differentiate metastatic from non-metastatic nodes, its sensitivity was found to be 100 %, specificity was 72.1 %, positive predictive value was 9.7 %, negative predictive value was 100 % and accuracy was 72.9 % for reader 1; 85.7 %, 90.6 %, 21.4 %, 99.5 % and 90.4 % for reader 2, in this case with a cutoff value of 0.904×10^{-3} mm^2/s.

Using the minimum ADC region value for the same purpose, with a cutoff of 0.807×10^{-3} mm^2/s (reader 1), the diagnostic performance increased in all indices with respect to the mean ADC region value. Sensitivity was found to be 100 %, specificity was 98.3 %, positive predictive value was 63.6 %, negative predictive value was 100 % and accuracy was 98.3 % for the first reader. For the 0.798 (10^{-3} mm^2/s) cutoff of reader 2, the corresponding results were: 100 %, 99.6 %, 87.5 %, 100 % and 99.6 %.

Regarding the standard size criteria, using a short axis diameter >10 mm to distinguish between benign and malignant nodes [6, 23, 24], the indices of diagnostic performance were generally inferior to those obtained with ADC measurements (Table 4).

Discussion

The differentiation between benign and malignant nodes is essential for staging, therapy planning and follow-up of a primary carcinoma [16]. Conventional MR techniques are commonly used in the evaluation of pelvic nodes in patients with gynaecologic malignancy [19], defining as metastatic those nodes with short-axis diameter >10 mm [23] or

Table 3 Description of the mean and minimum ADC values of regions with histopatological results, by metastatic status

DWI region based parameters	Non-metastatic regions				Metastatic regions				p-value*
	No.	Average	SD	1st–3rd quartiles	*No.*	Average	SD	1st–3rd quartiles	
ADC mean (10^{-3} mm^2/s)									
- Reader 1	89	1.07	0.20	0.92–1.18	7	0.87	0.15	0.78–0.95	0.0103
- Reader 2	87	1.05	0.16	0.91–1.16	7	0.84	0.13	0.74–0.90	0.0010
ADC minimum (10^{-3} mm^2/s)									
- Reader 1	89	1.02	0.20	0.90–1.10	7	0.74	0.07	0.70–0.79	0.0004
- Reader 2	87	1.00	0.16	0.88–1.10	7	0.74	0.04	0.70–0.77	<0.0001

*p-values for comparison of ADC values are based on the t-test for each ADC summary measure and for each reader

SD, standard deviation

>8 mm [16]. However, based only on this size criteria, the sensitivity in the diagnosis of metastatic nodes remains low (25–62 %) [6, 25], despite higher specificities (93 %–97 %) [6, 24]. Moreover, Williams et al. [26] reported that, of 504 nodes in 18 patients with gynaecologic malignancy, 54.5 % of 34 metastatic nodes were <10 mm in length. Also when considering the short-to-long axis ratio (cutoff value: 0.77), the sensitivity and specificity of the MR examination remained low (56.1 % and 71.3 %) [21].

DWI, by reflecting changes in proton mobility [27], may allow distinguishing cancerous from normal tissues [28] as malignant tissues present with higher signal intensity and lower ADC values than normal tissues or benign lesions [6, 27, 29–35]. In particular, for patients with endometrial cancer, it has recently been suggested [36, 37] that DW imaging may be superior to conventional MR techniques in assessing the overall stage of disease, in particular regarding the depth of myometrial invasion.

Ichikawa et al. [38] reported that, in patients with colorectal cancer, metastatic and non-metastatic nodes were similarly visualised as high-signal intensity regions on DW images. Conversely, previous studies on patients with head and neck cancers have reported that DW images and ADC maps can differentiate metastatic from benign cervical lymph nodes with high accuracy, even if with discordant results. Sumi et al. [13] found higher ADC values for metastatic than for benign nodes, whereas other authors [14, 15] reported lower ADC values for malignant than for benign nodes.

Recently, the reliability of DW images and ADC measurements in the evaluation of nodal status in patients with endometrial and cervical cancer has been investigated, with discrepancies among results [6, 16, 18–20]. Moreover, to our knowledge, our study is the first one performed in a more homogeneous study population, since it includes only patients with endometrial cancer.

In our study, at qualitative evaluation of DWIBS images, both metastatic and non-metastatic nodes presented with high signal intensity [16, 20, 38].

As for the quantitative analysis of ADC values, on a region-based analysis, we found significantly lower ADC values for metastatic than for non-metastatic pelvic sites, as in other studies recently performed in patients with uterine cervical cancer [18, 20]. This could be due to increased cellularity and enlarged cell size, and to the presence of enlarged nuclei, hyperchromatism and high nuclear-to-cytoplasm ratio in cancerous cells that reflect in restricted motion of extracellular and intracellular water molecules [20].

Moreover, the absolute average difference between normal and metastatic nodes in mean and minimum ADC regions values exceeded the limits of interobserver agreements, contrary to what was reported by Kwee et al. [39] indicating that ADC measurements are sufficiently reproducible to differentiate between malignant and non malignant lymph nodes.

Mean and minimum ADC values were found to be reliable diagnostic tools not only on a region-based analysis, indicating which specific nodal region is involved, but also on a patient-based analysis, indicating which patients should undergo pelvic lymphadenectomy (sensitivity=100 %, specificity >94.1 % for miminim ADC). Differential diagnosis between benign and malignant lymph nodes with short-axis diameter <10 mm is always difficult in diagnostic imaging [18]. In our study, among

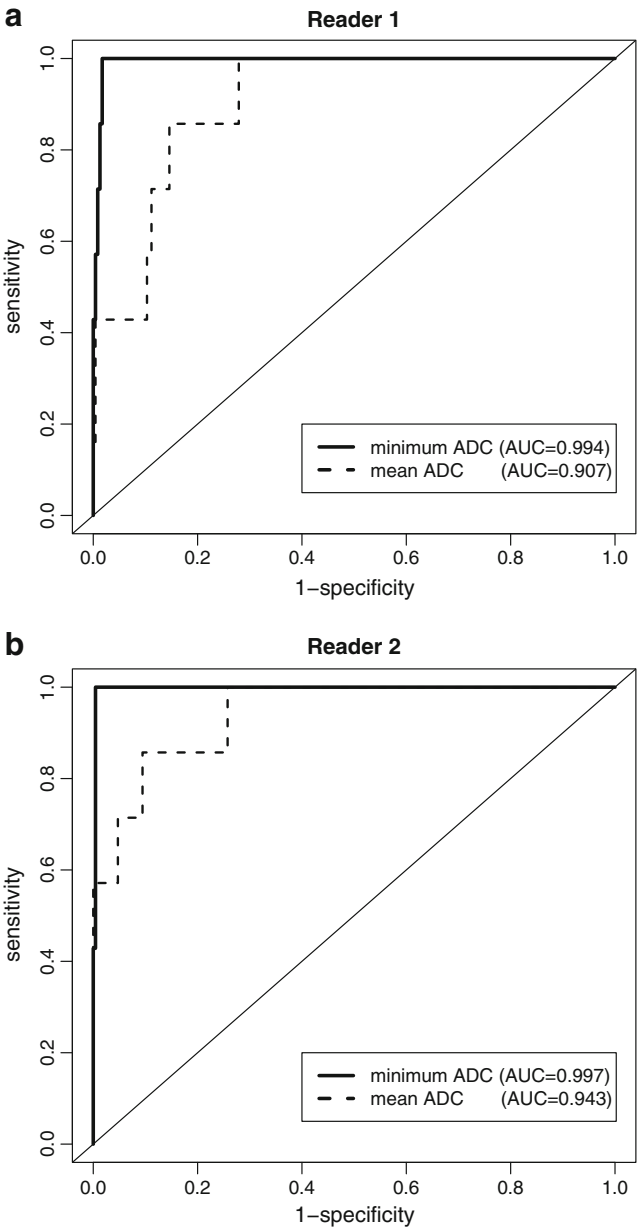

Fig. 4 **a**–**b**: ROC curves that differentiate metastatic from non-metastatic regions using the mean (dashed line) or the minimum (solid line) ADC values with reference to histopathological and follow-up findings (n=240), by reader. The AUCs of both markers are reported in the legend

15 metastatic nodes, only 5 (33.3 %) had a short-axis diameter >10 mm. When using this cutoff value (short axis diameter >10 mm) to predict lymph nodal involvement, we found a low sensitivity value, despite of higher specificity, in line with results of other studies, even if different methods of nodal analysis were adopted, such as considering only nodes with a short-axis diameter >5 mm, or using as diagnostic criteria the shape (round) and margins (spiculated) in addition to the size (short-axis diameter >8 mm) [6, 16, 20, 24, 40]. In our series, the diagnostic performance of ADC values was much higher than that of standard size criteria, as Liu et al. already found in patients with cervical cancer [20]. For the reasons reported above, in particular considering the tendency towards lower ADC values in malignant nodes, our results were even better when referring to the minimum than to the mean ADC region value. These results are in keeping with findings of previous authors [18, 20] and indicate that DWI has the potential ability to provide functional information regarding microstructure changes, which may precede significant size alterations, thus allowing the radiologist to detect metastatic nodes that are not enlarged [20]. Moreover, the cutoff of minimum ADC region values obtained from the two different readers were more similar than the cutoff of mean ADC values. This means that the minimum ADC value may represent a more reproducible and therefore effective tool in differentiating metastatic from non-metastatic pelvic nodal stations.

We acknowledge that our study has some limitations. Firstly, the patient population considered was relatively small, with a low prevalence of metastatic pelvic nodes, thus resulting in rather low positive predictive values and wider confidence intervals in this parameter and in sensitivity. Secondly, like in the majority of published studies on endometrial cancer patients, our results were obtained with a 1.5-T MR system; it cannot be ruled out that MRI at higher magnetic field (3 T) could even improve results. Thirdly, the low spatial resolution of DWIBS MR acquisition in our study would account for a number of small nodes being missed and for possible inaccurate ADC measurements for small nodes, given potential partial volume averaging effects. Fourthly, the retrospective nature of the study didn't allow us to precisely match the histopathological to the MR findings of each single node, but we took this into account, performing a per-region analysis, which is also more useful from a clinical perspective.

In conclusion, DW MR imaging seems to be a promising diagnostic tool for demonstrating the presence of pelvic metastases in patients with endometrial cancer, since ADC values of metastatic nodal sites are significantly lower than those of normal ones, with a high reproducibility. In addition, the minimum ADC region value is more appropriate than the mean ADC region value to assess the suspicion of metastases and we believe that it is easier to apply in the clinical practice.

Table 4 Diagnostic performance of ADC region summary values and T2-weighted size criteria with reference to histopathological and follow-up findings (n=240)

Diagnostic index	ADC-based				T2-based			
	Mean*		Minimum#		Short axis		Short-to-long axis ratio	
	Estimate	(95 % CI)	Estimate	(95 % CI)	Estimate	(95 % CI)	Estimate	(95 % CI)
Sensitivity (%)								
- Reader 1	100.0	(64.6–100.0)	100.0	(64.6–100.0)	28.6	(8.2–64.1)	42.9	(15.8–75.0)
- Reader 2	85.7	(48.7–97.4)	100.0	(64.6–100.0)	14.3	(2.6–51.3)	28.6	(8.2–64.1)
Specificity (%)								
- Reader 1	72.1	(66.0–77.5)	98.3	(95.7–99.3)	87.1	(82.2–90.8)	92.3	(88.1–95.1)
- Reader 2	90.6	(86.1–93.7)	99.6	(97.6–99.9)	87.1	(82.2–90.8)	91.9	(87.6–94.7)
PPV (%)								
- Reader 1	9.7	(4.8–18.7)	63.6	(35.4–81.8)	6.3	(1.7–20.2)	14.3	(5.0–34.6)
- Reader 2	21.4	(10.2–39.5)	87.5	(52.9–97.8)	3.2	(0.6–16.2)	9.5	(2.7–28.9)
NPV (%)								
- Reader 1	100.0	(97.8–100.0)	100.0	(98.4–100.0)	97.6	(94.5–99.0)	98.2	(95.4–99.3)
- Reader 2	99.5	(97.4–99.9)	100.0	(98.4–100.0)	97.1	(93.9–98.7)	97.7	(94.8–99.0)
Accuracy (%)								
- Reader 1	72.9	(65.2–79.4)	98.3	(94.7–99.5)	85.4	(80.4–89.3)	90.8	(86.5–93.9)
- Reader 2	90.4	(86.0–93.5)	99.6	(96.7–99.9)	85.0	(79.9–89.0)	90.0	(85.6–93.2)

*Cutoff values for mean ADC are 1.092 and 0.9041 for reader 1 and 2, respectively

#Cutoff values for minimum ADC are 0.8077 and 0.7982 for reader 1 and 2, respectively

References

1. Ayhan A, Tuncer R, Tuncer ZS, Yuce K, Kucukali T (1994) Correlation between clinical and histopathologic risk factors and lymph node metastases in early-endometrial cancer (a multivariate analysis of 183 cases). Int J Gynecol Cancer 4:306–309
2. Lutman CV, Havrilesky LJ, Cragun JM et al (2006) Pelvic lymph node count is an important prognostic variable for FIGO stage I and II endometrial carcinoma with high-risk histology. Gynecol Oncol 102:92–97
3. Kodama J, Seki N, Nakamura K, Hongo A, Hiramatsu Y (2007) Prognostic factors in pathologic parametrium-positive patients with stage IB-IIB cervical cancer treated by radical surgery and adjuvant therapy. Gynecol Oncol 105:757–761
4. Choi HJ, Kim SH, Seo SS et al (2006) MRI for pretreatment lymph node staging in uterine cervical cancer. AJR Am J Roentgenol 187:538–543
5. Kim JH, Beets GL, Kim MJ et al (2004) High-resolution MR imaging for nodal staging in rectal cancer: are there any criteria in addition to the size? Eur J Radiol 52:78–83
6. Lin G, Ho K-C, Wang J-J et al (2008) Detection of lymph node metastasis in cervical and uterine cancers by diffusion-weighted magnetic resonance imaging at 3 T. J Magn Reson Imaging 28:128–135
7. Eiber M, Beer AJ, Holzapfel K et al (2010) Preliminary results for characterization of pelvic lymph nodes in patients with prostate cancer by diffusion-weighted MR-imaging. Investig Radiol 45:15–23
8. Rechichi G, Galimberti S, Signorelli M et al (2011) Endometrial cancer: correlation of apparent diffusion coefficient with tumour grade, depth of myometrial invasion and presence of lymph node metastases. AJR Am J Roentgenol 197:256–262
9. Thoeny HC, De Keyzer F (2007) Extracranial applications of diffusion weighted magnetic resonance imaging. Eur Radiol 17:1385–1393
10. Szafer A, Zhong J, Anderson AW, Gore JC (1995) Diffusion-weighted imaging in tissues: theoretical models. NMR Biomed 8:289–296
11. Guo Y, Cai YQ, Cai ZL et al (2002) Differentiation of clinically benign and malignant breast lesions using diffusion-weighted imaging. J Magn Reson Imaging 16:172–178
12. Rubesova E, Grell AS, De Maertelaer V, Metens T, Chao SL, Lemort M (2006) Quantitative diffusion imaging in breast cancer: a clinical prospective study. J Magn Reson Imaging 24:319–324
13. Sumi M, Cauteren MV, Nakamura T (2006) MR microimaging of benign and malignant nodes in the neck. AJR Am J Roentgenol 186:749–757
14. Holzapfel K, Duetsch S, Fauser C, Eiber M (2009) Value of diffusion-weighted MR imaging in the differentiation between benign and malignant cervical lymph nodes. Eur J Radiol 72:381–387
15. Razek A, Soliman NY, Elkharaway S, Tawfik A (2006) Role of diffusion weighted MR imaging in cervical lymphadenopathy. Eur Radiol 16:1468–1477 (Rev 1; [15])
16. Roy C, Bierry G, Matau A, Bazille G, Pasquali R (2010) Value of diffusion-weighted imaging to detect small malignant pelvic lymph nodes at 3 T. Eur Radiol 20:1803–1811
17. Beer AJ, Eiber M, Souvatzoglou M et al (2011) Restricted water diffusibility as measured by diffusion-weighted MR imaging and choline uptake in 11C-choline PET/CT are correlated in pelvic lymph nodes in patients with prostate cancer. Mol Imaging Biol 13:352–361
18. Chen YB, Hu CM, Chen GL, Hu D, Liao J (2010) Staging of uterine cervical carcinoma: whole-body diffusion-weighted magnetic resonance imaging. Abdom Imaging 36:619–626
19. Nakai G, Matsuki M, Inada Y et al (2008) Detection and evaluation of pelvic lymph nodes in patients with gynecologic malignancies using body diffusion-weighted magnetic resonance imaging. J Comput Assist Tomogr 32:764–768
20. Liu Y, Liu H, Bai X et al (2011) Differentiation of metastatic from non-metastatic lymph nodes in patients with uterine cervical cancer using diffusion-weighted imaging. Gynecol Oncol 122:19–24
21. Chen YB, Liao J, Xie R, Chen GL, Chen G (2011) Discrimination of metastatic from hyperplastic pelvic lymph nodes in patients with cervical cancer by diffusion-weighted magnetic resonance imaging. Abdom Imaging 36:102–109 (Rev 1; [21])
22. Brown LD, Cai TT, Das Gupta A (2001) Interval estimation for a binomial proportion. Stat Sci 16:101–133
23. Kim SH, Kim SC, Choi BI et al (1994) Uterine cervical carcinoma: evaluation of pelvic lymph node metastasis with MR imaging. Radiology 190:807–811
24. Choi HJ, Kim SH, Seo SS et al (2003) MRI for pretreatment lymph node staging in uterine cervical cancer. AJR Am J Roentgenol 187: W538–W543
25. Nakai G, Matsuki M, Inada Y et al (2008) Feasibility of diffusion-weighted (Rev 1; [25]) imaging in the differentiation of metastatic from nonmetastatic lymph nodes: early experience. J Magn Reson Imaging 28:714–719
26. Williams AD, Cousins C, Soutter WP et al (2001) Detection of pelvic lymph node metastases in gynecologic malignancy: a comparison of CT, MR imaging, and positron emission tomography. AJR Am J Roentgenol 177:343–348
27. Shen SH, Chiou YY, Wang JH et al (2008) Diffusion-weighted single-shot echo-planar imaging with parallel technique in assessment of endometrial cancer. AJR Am J Roentgenol 190:481–488
28. Patterson DM, Padhani AR, Collins DJ (2008) Technology insight: water diffusion MRI—a potential new biomarker of response to cancer therapy. Nat Clin Pract Oncol 5:220–233
29. Ichikawa T, Haradome H, Hachiya J et al (1998) Diffusion-weighted MR imaging with a single-shot echoplanar sequence: detection and characterization of focal hepatic lesions. AJR Am J Roentgenol 170:397–402
30. Kim T, Murakami T, Takahashi S et al (1999) Diffusion-weighted single-shot echoplanar MR imaging for liver disease. AJR Am J Roentgenol 173:393–398
31. Shimofusa R, Fujimoto H, Akamata H et al (2005) Diffusion-weighted imaging of prostate cancer. J Comput Assist Tomogr 29:149–153
32. Thoeny HC, Keyzer FD, Oyen RH et al (2005) Diffusion-weighted MR imaging of kidneys in healthy volunteers and patients with parenchymal diseases: initial experience. Radiology 235:911–917
33. Naganawa S, Sato C, Kumada H et al (2005) Apparent diffusion coefficient in cervical cancer of the uterus: comparison with the normal uterine cervix. Eur Radiol 15:71–78
34. Sato C, Naganawa S, Nakamura T et al (2005) Differentiation of non-cancerous tissue and cancer lesions by apparent diffusion coefficient values in transition and peripheral zones of the prostate. J Magn Reson Imaging 21:258–262
35. Inada Y, Matsuki M, Nakai G et al (2007) Body diffusion-weighted MR imaging of uterine endometrial cancer: is it helpful in the detection of cancer in nonenhanced MR imaging? Eur J Radiol 17:201–204
36. Beddy P, Moyle P, Kataoka M et al (2012) Evaluation of depth of myometrial invasion and overall staging in endometrial cancer: comparison of diffusion-weighted and dynamic contrast-enhanced MR imaging. Radiology 262:530–537
37. Rechichi G, Galimberti S, Signorelli M, Perego P, Valsecchi MG, Sironi S (2009) Myometrial invasion in endometrial cancer:

diagnostic performance of diffusion-weighted MR imaging at 1.5-T. Eur Radiol 20:754–762
38. Ichikawa T, Erturk SM, Motosugi U et al (2006) High-b-value diffusion-weighted MRI in colorectal cancer. AJR Am J Roentgenol 187:181–184
39. Kwee T, Takahara T, Luijten PR, Nievelstein RAJ (2010) ADC measurements of lymph nodes: inter- and intra-observer reproducibility study and an overview of the literatue. Eur J Radiol 75:215–220
40. Choi HJ, Roh JW, Seo SS et al (2006) Comparison of the accuracy of magnetic resonance imaging and positron emission tomography/computed tomography in the presurgical detection of lymph node metastases in patients with uterine cervical carcinoma: a prospective study. Cancer 106:914–922